研 究 解 説

Modeling Masonry Structures using the Applied Element Method

Paola MAYORCA* and Kimiro MEGURO**

INTRODUCTION

Masonry is one of the oldest construction materials which is presently in use. Thirty per cent of the world current population lives in a home of unbaked earth, which is one unreinforced masonry type. These structures are extremely vulnerable during earthquakes and their collapse is one of the main causes of casualties during these events. Thus, it is necessary to evaluate its seismic performance and eventually devise countermeasures.

Masonry varies worldwide, not only due to the different characteristics of its components, brick and mortar, but also to different construction practices. The great variability of the material together with limited economic resources make it difficult to carry out experimental studies for all types of existing masonry. The numerical approach is a powerful tool to overcome this situation.

There are three approaches for the numerical modeling of masonry structures: detailed micro modeling, simplified micro modeling[1,2], and macro modeling[3,4]. In this study, simplified micro modeling is adopted because it allows a degree of detail sufficient to discuss masonry vulnerability and to design countermeasures. In this approach, mortar and brick properties are combined. In spite of this, the brick arrangement is kept as an input variable of the analysis. Thus, walls with discontinuities, such as windows and door openings, can be analyzed.

The analysis is performed with the Applied Element Method (AEM) because it can simulate structural behavior from early stages of loading until total collapse. The feature that makes this technique especially suitable for masonry analysis is that it can follow crack formation and propagation without any crack location presumption. The general formulation of the AEM is discussed elsewhere[5]. Only the issues directly related to masonry modeling are presented in this paper. Further details may be found in Mayorca[6].

* Institute of Industrial Science, University of Tokyo, Postdoctoral Fellow
** Institute of Industrial Science, University of Tokyo, Associate Professor

APPLIED ELEMENT METHOD FOR MASONRY MODELING

Two types of springs are needed: brick and brick-mortar spring, to model masonry in the AEM. The former connects elements inside a single brick whereas the later connects elements belonging to different bricks and therefore includes the mortar interface.

The brick spring stiffness is calculated following the formulation presented in Tagel-Din and Meguro[5] as it connects elements of identical materials. For the brick-mortar springs, on the other hand, equivalent normal and shear stiffness are considered

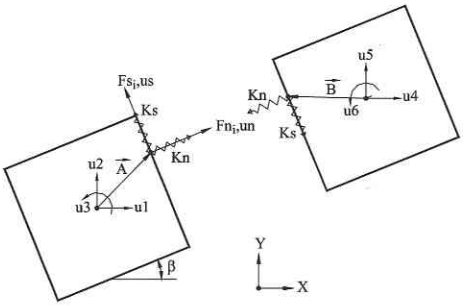

(a) Applied Element Method principle

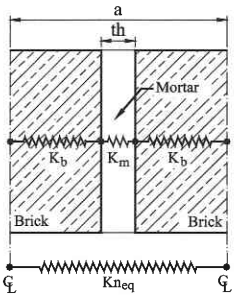

(b) Brick-mortar spring

Figure 1 Masonry modeling in the Applied Element Method

assuming a system of brick and mortar springs arranged in series as shown in Figure 1. The equivalent stiffness is:

$$\frac{1}{Kn_{eq}} = \frac{a-th}{E_b \times t \times d} + \frac{th}{E_m \times t \times d} \quad \cdots\cdots (1)$$

$$\frac{1}{Ks_{eq}} = \frac{a-th}{G_b \times t \times d} + \frac{th}{G_m \times t \times d} \quad \cdots\cdots (2)$$

where E_b and G_b are the brick Young and shear modulus, similarly E_m and G_m for the mortar and t is the element thickness. Other symbols are shown in Figure 1.

MATERIAL MODEL

Modeling masonry components separately is not applicable to the approach adopted in this study. For the simplified micro modeling, the interaction between components must be reflected in the constitutive law. Five failure types are observed in masonry walls: (1) joint debonding, (2) sliding along the bed or head joints, (3) cracking of units under direct tension, (4) diagonal tensile cracking of the units under high compression and shear, and (5) "masonry crushing", which is actually splitting of bricks. It is clear that (1) and (2) should be reflected in the brick-mortar springs and (3) and (4), in the brick springs. To include (5) without considering the interaction between mortar and brick explicitly, a compression cap limiting the brick-spring compression stresses may be included[1].

The three phenomena relevant to the brick mortar springs can be considered in the framework of plasticity. Each failure mode is associated with one failure surface as shown in Figure 2. In the present study, the inclusion of the compression cap was considered unnecessary. In unreinforced masonry houses subjected to seismic excitations, the structure boundary and loading conditions seldom cause masonry compression failure. Tension and shear sliding are dominant in the behavior.

The failure surfaces used for the tension cut-off and Coulomb friction are simplifications of the ones proposed in Lourenço[1]. The tension cut-off yield function is given by:

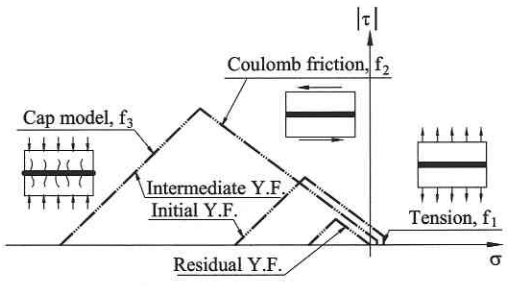

Figure 2 Brick-mortar spring yield surface

$$f_1(\boldsymbol{\sigma}, \kappa_1) = \sigma - \bar{\sigma}_1 \quad \cdots\cdots (3)$$

The yield value is given by:

$$\bar{\sigma}_1 = \begin{cases} f_t\left(1 - \dfrac{f_t}{G_f^I}\kappa_1\right) & , \ \kappa_1 \le \dfrac{2G_f^I}{f_t} \\ 0 & , \ \kappa_1 > \dfrac{2G_f^I}{f_t} \end{cases} \quad \cdots\cdots (4)$$

where f_t is the bond strength, κ_1, the relevant hardening parameter, and G_f^I, the Mode I fracture energy.

For the Coulomb friction criterion, the yielding function is:

$$f_2(\boldsymbol{\sigma}, \kappa_2) = |\tau| - \sigma \tan\phi - \bar{\sigma}_2 \quad \cdots\cdots (5)$$

and the yielding value is:

$$\bar{\sigma}_2 = \begin{cases} c\left(1 - \dfrac{c}{G_f^{II}}\kappa_2\right) & , \ \kappa_2 \le \dfrac{2G_f^{II}}{c} \\ 0 & , \ \kappa_2 > \dfrac{2G_f^{II}}{c} \end{cases} \quad \cdots\cdots (6)$$

where c is the joint cohesion, κ_2, the relevant hardening parameter, G_f^{II}, the Mode II fracture energy, and ϕ, the friction angle. The non-associated flow rule is:

$$g_2 = |\tau| - c \quad \cdots\cdots (7)$$

Although mortar interfaces exhibit dilatancy when sheared, this effect is not taken into account in the present model.

The cohesion and tension softening are assumed coupled and the composite yielding surface is assumed to isotropically soften, i.e. the yielding surfaces f_1 and f_2 shrink simultaneously towards the origin and reach it concurrently[1]. Although there is no experimental data confirming this supposition, it is reasonable to assume that the tension and cohesion strengths are related and the degradation in one results in the degradation of the other.

The phenomena relevant to the brick spring is modeled using the following expression for the brick failure envelope[7]:

$$\frac{f_b}{f'_b} + \left(\frac{f_t}{f'_t}\right)^{0.55} = 1 \quad \cdots\cdots (8)$$

where f_b and f_t are the principal compression and tensile stresses, respectively, and f'_b and f'_t are the uniaxial compression and tensile strengths, respectively. The spring principal stresses were calculated using the approach presented elsewhere[5].

MODEL VALIDATION

In order to test the model ability to simulate the behavior of walls, the tests carried out within the scope of the CUR project[8] were used. This testing program was extensively instrumented and

the material uniformity was given especial attention. The specimen dimensions are shown in Figure 3. The wall width was 100mm and the mortar thickness, 10mm.

At first, the wall was subjected to a vertical preload, p, while the upper horizontal beam was kept horizontal. After application of the vertical load, the upper beam was fixed and the shear test started. In order to keep the horizontality of the upper beam, the vertical load was adjusted. This loading and boundary conditions are hardly observed in the reality. However, for the purpose of verifying the numerical technique, this dataset was chosen.

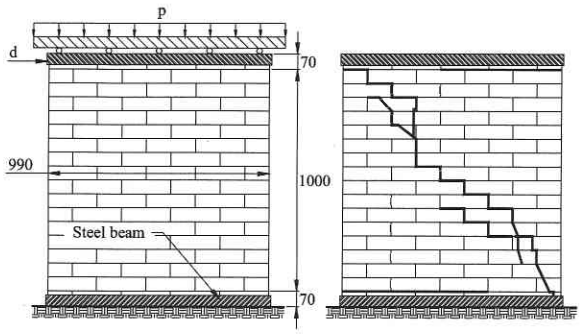

(a) Wall specimen dimensions　(b) Experimental crack patterns

Figure 3 Masonry wall dimensions (in mm) and crack pattern[8)]

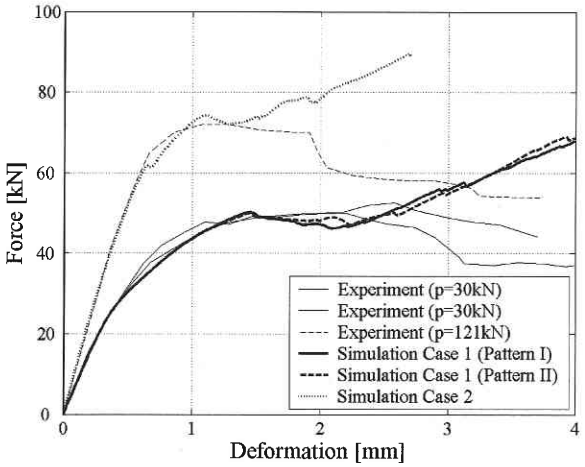

Figure 4 Force deformation curve

Two cases from the experimental program were simulated. The summary of the simulation conditions are shown in Table 1. The brick modulus of elasticity was obtained experimentally while the mortar modulus of elasticity was adjusted to fit the initial stiffness of the observed force-displacement curve.

In order to study the effect of the mesh refinement on the simulation results, two meshes, namely Pattern I and II, were considered for Case 1. Figure 4 shows the force deformation curves obtained in the simulation. The analysis results for the two considered patterns did not change considerably. However, the computational time was directed influenced. More elements implied more degrees of freedom increasing the stiffness matrix size and bandwidth.

In general, the simulation agrees very well with the first portion of the experimental curve. However, the agreement decreases in the later portion. The reason for this is that the compression cap was not included in the numerical model of the brick mortar spring. Due to the experimental boundary conditions, a diagonal compression strut develops along the loaded diagonal as the hor-

Table 1. Masonry material properties used in the analysis

Case	p (kN)	E_b (kN/mm^2)	E_m (kN/mm^2)	f_t (N/mm^2)	c (N/mm^2)	G_f^I (N×mm/mm^2)	G_f^{II} (N×mm/mm^2)	tanϕ
1	30	170.0	4.0	0.25	0.35	0.018	0.125	0.75
2	121	170.0	10.3	0.16	0.22	0.018	0.050	0.75

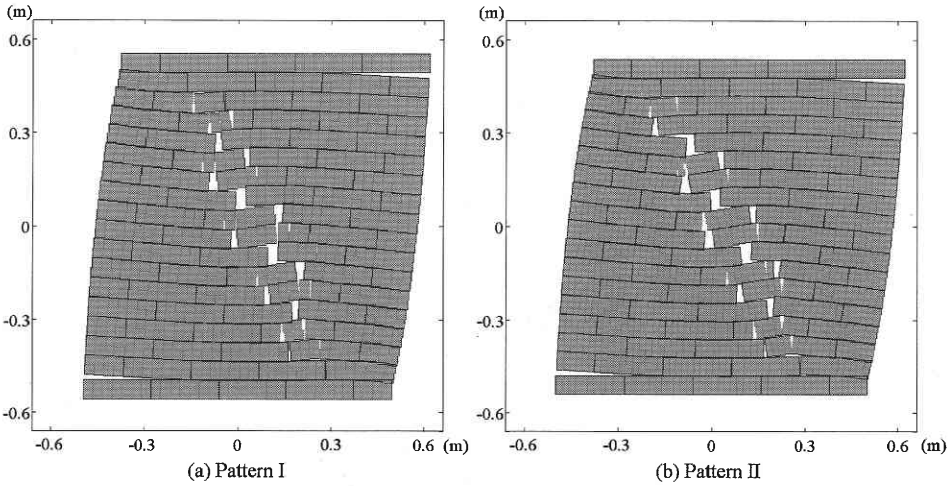

Figure 5 Deformed shape for different mesh refinements (Scale factor = 30)

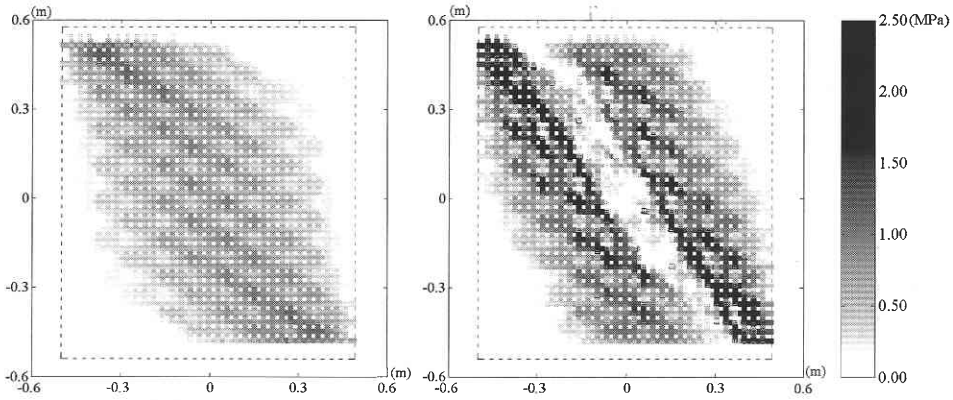

(a) Deformation=1mm (b) Deformation=4mm

Figure 6 Shear stress distribution (in MPa)

izontal deformation increases. Without the cap, the compression stresses in this region are unlimited. As a consequence, the shear strength from the friction mechanism is also unbounded.

Three mechanisms govern the masonry shear strength depending of the magnitude of the normal compression stresses. With relatively low stresses, the shear friction is predominant. As the stresses increase, the diagonal cracking of the units controls the behavior. For large normal stresses, the masonry crushing is critical. The first two mechanisms, which are dominant in structures subjected to seismic actions, were well captured by the model.

Figure 5 shows the deformed shapes for the two considered meshes. No major difference in the crack location is distinguished. The simulated crack pattern agrees well with the experimentally observed shown in Figure 3.

Figure 6 shows the shear stress distribution at two stages of the wall loading, before and after the diagonal crack. At first, there are only two cracks at the lower and upper most mortar layer and therefore stresses have been released in this zone. The rest of the wall, however, behaves fairly continuous. The compressed diagonal is clearly observed. As the deformation increases, the diagonal crack occurs. As a result, the applied load is transferred along two compression struts on both sides of the crack while stresses along the cracked interface are released.

CONCLUSIONS

The paper presents an extension of the Applied Element Method (AEM) for the analysis of unreinforced masonry structures. Two types of spring, i.e. brick and brick-mortar spring, were considered to model the masonry anisotropy. In the framework of elastoplasticity, a simplified constitutive model for masonry was adapted and implemented. The model was validated with shear wall experiment data. A good agreement was found in the force deformation curve and crack pattern.

Although a compression cap to limit the compression stresses in the brick mortar spring is not included in the formulation, the model suffices for the evaluation of masonry seismic vulnerability and countermeasure design.

(Manuscript received, October 14, 2003)

REFERENCES

1) Lourenço P. B., *Computational strategies for masonry structures*, Ph.D. Dissertation, Delft University of Technology, Delft, The Netherlands, 1996.
2) Gambarotta, L. and Lagomarsino, S., Damage models for the seismic response of brick masonry shear walls. Part I: The mortar joint model and its applications, *Earthquake Engineering and Structural Dynamics*, **26**, 1997, p. 423–439.
3) Anthoine, A., Derivation of the in-plane elastic characteristics of masonry through homogenization theory, *Int. J. Solids Structures*, **32-2**, 1995, p. 137–163.
4) Lofti, H. R. and Shing, P. B., An appraisal of smeared crack models for masonry shear wall analysis, *Computers & Structures*, **41–3**, 1991, p. 413–425.
5) Tagel-Din H. and Meguro K., Applied Element Method for simulation of nonlinear materials: theory and application for RC structures, *Struct. Engrg. /Earthquake Engrg.*, **17(2)**, 2000, p. 137s–148s.
6) Mayorca, P., *Strengthening of unreinforced masonry structures in earthquake prone regions*, PhD Dissertation, University of Tokyo, Japan, 2003.
7) Khoo, C. L. and Hendry, A. W., Strength tests of brick and mortar under complex stresses for the development of a failure criterion for brick work in compression, *Proc. British Ceramic Society*, **21**, 1973, p. 51–66.
8) Rajimakers, T. M. J. and Vermeltfoort, A. T., *Deformation controlled meso shear tests on masonry piers*, Rep. B–92–1156, TNO BOUW/TU Eindhoven, Build. and Constr. Res., Eindhoven, The Netherlands, 1992 (in Dutch).